Heliyon 9 (2023) e21235

Contents lists available at ScienceDirect

Heliyon

journal homepage: www.cell.com/heliyon

N-acetylcysteine attenuates the incidence of phlebitis induced by carbomer/vinorelbine gel

Hongyu Zhang [a,1], Jing Gong [a,1], Shiyu Zhang [b,1], Liwen Luo [c], Chengqin Luo [a], Ke Bi [a], Lei Wang [a], Xuewei Kan [d], Zhiqian Tian [b,*], Xiaolong Wang [a,**]

[a] Department of Emergency, The Second Affiliated Hospital of Chongqing Medical University, Chongqing, China
[b] Institute of Immunology, PLA, Army Medical University (Third Military Medical University), Chongqing, China
[c] Department of Orthopaedics, Xinqiao Hospital, Army Medical University (Third Military Medical University), Chongqing, China
[d] Department of Dermatology, First Affiliated Hospital of USTC, Division of Life Sciences and Medicine, University of Science and Technology of China, Hefei, Anhui, China

ARTICLE INFO

Keywords:
Phlebitis
Carbomer
N-acetylcysteine
Vinorelbine
Sustained-release carrier gel

ABSTRACT

Background: The high incidence and severe clinical manifestations of phlebitis pose a complex and urgent clinical challenge. The rapid and simple establishment of animal phlebitis models and the development of preventive strategies are crucial to resolving this problem.
Methods: In this study, we established such models by mixing vinorelbine ditartrate (VNR) and carbomer to form a sustained-release gel carrier, and then injected it around the veins rather than inside the vessels. Furthermore, we analyzed the efficacy of the carbomer/VNR gel in inducing phlebitis by monitoring the morphology of the veins using HE staining, immunohistochemical and immunofluorescence staining, and western blotting. Reactive oxygen species (ROS) and lipid peroxidation levels were determined using flow cytometry. Finally, we evaluated the inhibitory effect of N-acetylcysteine (NAC) on VNR-induced phlebitis in rabbits and rats.
Results: Our findings suggested that the carbomer/VNR gel rapidly and easily induced phlebitis due to by retention of the gel in situ, wrapping the veins, and the prolonged release of VNR. NAC alleviated the VNR-induced oxidative stress response and expression of inflammatory cytokines by attenuating mitochondrial damage in venous endothelial cells, thereby preventing the occurrence of phlebitis in rabbits and rats.
Conclusion: The in situ carbomer/VNR gel provides a rapid and simple method for establishing an animal model to study the pathogenesis of phlebitis. Furthermore, the observed therapeutic effect of NAC highlights its novel and efficacious role in preventing and treating phlebitis.

1. Introduction

Most patients with malignant tumors require chemotherapy [1]. Repeated intravenous injections of chemotherapy drugs lead to an

* Corresponding author. Institute of Immunology, PLA, Army Medical University (Third Military Medical University), 30 Gaotanyan St, Dist. Shapingba, Chongqing 400038, China.
** Corresponding author. Department of Emergency, The Second Affiliated Hospital of Chongqing Medical University, 76 Linjiang Road, Yuzhong District, Chongqing, 400000, China.
E-mail addresses: tzhiq009@tmmu.edu.cn (Z. Tian), wang.xiaolong@cqmu.edu.cn (X. Wang).
[1] These authors have contributed equally to this work.

https://doi.org/10.1016/j.heliyon.2023.e21235
Received 21 June 2023; Received in revised form 20 September 2023; Accepted 18 October 2023
Available online 24 October 2023

increased incidence of phlebitis, with a probability as high as 70 % [2]. Chemotherapeutic drugs circulate throughout the body owing to their fluidity [3], and their distribution can lead to systemic toxicity [4]. Patients with phlebitis typically do not exhibit systemic symptoms, but they do present local symptoms such as skin redness, pain, sclerosis, swelling, or venous thrombosis in severe cases [5,6]. Phlebitis severely affects the quality of life of patients and weakens the effects of subsequent chemotherapy [7]. Therefore, adequate measures must be developed to prevent and treat phlebitis.

Establishing an animal phlebitis model *in vivo* might help investigate the mechanism and pathological process of infusion phlebitis and aid in formulating effective prevention and treatment measures. The primary method of constructing an animal phlebitis model is the intravenous administration of chemotherapy drugs [6,8,9]. Multiple long-term chemotherapy injections at the infusion site are required to effectively induce phlebitis [10], which increases the difficulty of the procedure and reduces the probability of successful phlebitis induction. Furthermore, the venous diameter is reduced in rabbits, mice, and rats, complicating the chemotherapy drug injection. Notably, expertise is required to successfully construct animal phlebitis models that avoid multiple puncture-induced vascular damage [11,12]. Therefore, a simple, rapid, and local induction method for animal phlebitis models must be developed to overcome these limitations.

Vinorelbine (VNR) is a potent antitumor drug that increases the permeability of blood vessels, penetrates subcutaneous tissues, and accumulates locally, thereby causing local venous irritation or phlebitis during intravenous injection [13–17]. The incidence of local venous irritation or phlebitis after VNR injection from the peripheral superficial vein can be as high as 30 % [18]. To treat VNR-induced phlebitis, local treatment and systemic medication are typically used in combination, such as antipyretic and analgesic drugs to relieve pain, anticoagulant drugs to prevent the spread of the thrombus, and 50 % magnesium sulfate wet compression and external ointment to reduce symptoms [11,19,20]. Although the aforementioned treatment methods have certain therapeutic effects, the prevention and radical treatment of chemotherapeutic phlebitis have minimal effects. VNR could also cause mitochondrial function injury, increase the level of reactive oxygen species (ROS) in endothelial cells, and promote the expression of inflammatory cytokines IL-6, TNF-α, and IL-1β, and thus causing vascular endothelial injury or infusion phlebitis [8,16,21]. Therefore, the focus of the current study was to identify effective measures to prevent phlebitis and relieve its clinical symptoms via the reduction of VNR-induced mitochondrial function injury.

Carbomer 940 (carbomer), a crucial rheological regulator and excellent gel substrate at PH 7.0 [22], is stable and safe, and is often used to synthesize pastes and gels [23]. We speculated that combined with the high induction rate of VNR-induced phlebitis and the rheological properties of carbomer, VNR and carbomer could be mixed to form a gel that could be injected and retained in situ to stimulate veins, thus providing an efficient and simple way to induce phlebitis. Therefore, we developed an animal model of phlebitis with the carbomer/VNR sustained-release gel. The gel was injected around the veins to prolong the release of VNR, continuously stimulate the veins, and rapidly and locally induce phlebitis. It succeeded in this, thus allowing us to use the gel to explore the pathogenesis of phlebitis and develop prevention strategies. Along this line, we investigated the effect of NAC in mitigating infusion phlebitis. N-acetylcysteine (NAC), an antioxidant that penetrates cell membranes [24], can reduce ROS levels and relieve endothelial cell damage [21,25], but its effect on phlebitis prevention and treatment has not previously been investigated. In this study, NAC attenuated VNR-induced mitochondrial damage and inhibited phlebitis occurrence, which indicated that NAC could be administered in advance or simultaneously with chemotherapy drugs to prevent or treat phlebitis in clinical practice. We believe our study identifies a rapid and simple method to develop an animal phlebitis model for studying the underlying pathological mechanisms, which can assist in designing strategies to effectively reverse the symptoms and treat phlebitis.

2. Materials and methods

2.1. Reagents and antibodies

Vinorelbine ditartrate (VNR) (cat. No. V57040) was purchased from Acmec Biochemicals (Shanghai, China). N-acetylcysteine (NAC) amide (cat. No. T5518-2) was provided by TargetMol (Shanghai, China). Collagenase D (cat. No. 11088858001) was purchased from Sigma-Aldrich (St. Louis, Missouri, USA). Type II collagenase (cat. No. A004174) was obtained from Sangon Biotech (Shanghai, China). Carbomer 940 (cat. No. C7650), a hematoxylin-eosin (HE) stain kit (cat. No. G1120), and neutral balsams (cat. No. G8590) were obtained from Solarbio LIFE SCIENCES (Beijing, China). ROS Stain Kit (cat. No. BB-470513-200T) was purchased from BestBio (Shanghai, China). RIPA (cat. No. P0013B), PMSF (cat. No. ST506), and 5 × SDS-PAGE sample loading buffer (cat. No. P0015) were purchased from Beyotime Biotechnology (Shanghai, China). Anti-IL-6 antibody (cat. no.21865-1-AP), anti-CD31 antibody (cat. no.66065-2-Ig), anti-GPX4 antibody (cat. no.67763-1-Ig), anti-PINK1 antibody (cat. no.23274-1-AP) and anti-GAPDH antibody (cat. no.10494-1-AP) were obtained from Proteintech (Wuhan, China). Anti-IL-1β antibody (cat. No.bs-0812R) was obtained from Bioss (Beijing, China). Anti-TNF-α antibody (cat. No.sc-12744) was purchased from Santa Cruz Biotechnology (Dallas, TX, USA). Goat anti-rabbit IgG (Alexa Fluor® 594) (cat. No. ab150080) and goat anti-mouse IgG antibodies (Alexa Fluor® 488) (cat. No. ab150113) were purchased from Abcam (Cambridge, Massachusetts, USA).

2.2. Isolation of venous endothelial cells (VECs)

Three-week-old rats were anesthetized with 3 % pentobarbital sodium (50 mg/kg) and euthanized by cervical dislocation. After soaking in 75 % alcohol for 2–5 min, the rats were washed 2–3 times with PBS buffer. The abdominal cavity was opened as long as possible to expose and sever the inferior vena cava. The endothelium of the inferior vena cava was turned inside-out and digested with 2 % collagenase D and 2 % collagenase type II at 37 °C for 1–2 h. After blowing for 1 min, the inferior vena cava was discarded. The

remaining cell suspension was collected, and the VEC precipitate was obtained by centrifugation at 300×*g* for 5 min. VECs were inoculated at 5 % CO_2 and 37 °C and identified after cell fusion to 80–90 %.

2.3. Hematoxylin and eosin (HE) staining

The paraffin-embedded sections were deparaffinized for hydration. The sections were stained with hematoxylin and eosin for 3–5 min and 1–2 min, respectively. They were then washed thrice with PBS for 5 min each. After drying, the sections were sealed with neutral balsams and visualized using an M8 digital scanning microscopy imaging system (Precipoint/M8, Germany).

2.4. Immunofluorescence and immunohistochemistry

The paraffin-embedded sections were deparaffinized for hydration. The tissue sections and venous endothelial cells were fixed in 4 % paraformaldehyde. After washing with PBS, the samples were incubated with 3 % H_2O_2 for 30 min at 20–30 °C. Trypsin antigen repair solution was used for antigen repair. After washing with PBS, tissue sections or cells were sealed with goat serum at 20–30 °C for 30 min. Diluted first antibody (1:100) was added to the samples and incubated overnight at 4 °C. On the second day, the samples were washed thrice with PBS for 5 min each. For the immunofluorescence assay, diluted goat anti-rabbit IgG antibody (1:300) and goat anti-mouse IgG antibody (1:300) were added to the samples and incubated for 1–2 h at 37 °C. After washing with PBS, the samples were incubated with DAPI staining solution for 5 min and imaged using a fluorescence microscope (OLYMPUS, Japan). For the immunohistochemistry assay, the HRP-conjugated secondary antibody was added to the samples and incubated at 37 °C for 10–20 min. After washing with PBS, the samples were stained with DAB staining reagent and imaged using an M8 digital scanning microscopic imaging system.

2.5. Western blotting

After the tissues or cell precipitates were collected, RIPA buffer containing the protease inhibitor PMSF was added, and total proteins were cleaved and extracted. We added 5 × SDS-PAGE sample loading buffer in proportion to the sample volume. The sample was then boiled in water for 5 min. Subsequently, gel electrophoresis was performed under conditions of 60 V for 30–50 min and, subsequently, at 120 V for 60 min. After gel electrophoresis, the proteins were transferred to the PVDF membrane at 300 mA for 60 min. The PVDF membranes were incubated with 5 % milk powder for 1 h and washed thrice with Tris-buffered saline-Tween 20 (TBST) buffer for 5 min each. Subsequently, the membranes were incubated with diluted first antibody (1:1000) at 4 °C in a shaker overnight. The following day, the PVDF membrane was washed thrice with TBST buffer for 5 min each and incubated with diluted second antibody (1:5000) at 25 °C for 60 min with shaking. After washing, a super-sensitivity ECL kit (cat. No. BG0001, BIOGROUND, Chongqing, China) was used to image the PVDF in the ChemiDocTM Touch Imaging System (Bio-Rad, USA).

2.6. Cell viability assay

Cell viability was analyzed using the Cell Counting Kit (CCK-8) (cat. no. IV08-1000T, Invigentech™, California, USA). An appropriate number of cells were seeded in 96-well plates and incubated for 24 h. To determine the effect of NAC on cell proliferation, VECs were incubated again for 24 h at different concentrations of NAC. Then, 10 μl of CCK-8 reagent was added, and the cells were incubated at 37 °C in the dark for 2–5 h. After the incubation, the proliferation level of the cells was detected at 450 nm and statistically analyzed.

2.7. Flow cytometry

The VECs were trypsinized and isolated. The cell precipitates were collected by centrifugation at 300×*g* for 5 min, resuspended, and then incubated with diluted CD31 antibody (1:200) for 60 min at 37 °C. They were subsequently incubated with goat anti-mouse IgG antibody for 60 min at 37 °C, or the cell precipitates were resuspended with 500 μL of JC-1 working solution and incubated at 37 °C for 20 min. After incubation, the cells were collected by centrifugation at 300×*g* for 5 min. The cell precipitates were resuspended in PBS buffer or 1 × JC-1 assay buffer and assayed using flow cytometry (Beckman, USA). An apoptosis detection kit (cat. no. PI0100, Invigentech™, California, USA) was used for the detection of apoptosis rates. VECs were treated with various concentrations of NAC (0, 200, 400, 600 or 1000 μM) for 24 h. After collecting and washing with PBS, the cells were stained with 5 μl of Annexin V-FITC and 10 μl of PI in the dark for 10–20 min. After washing with PBS, the cells were analyzed by flow cytometry (Beckman, USA).

2.8. Glutathione (GSH) and malondialdehyde (MDA) assay

GSH and MDA levels in the VECs were detected using a GSH Colorimetric Assay Kit (cat. no. E-BC-K030-M), and a MDA Colorimetric Assay Kit (cat. no. E-BC-K028-M) obtained from Elabscience Biotechnology (Wuhan, China). The VECs were then collected and washed with PBS. For the GSH assay, after ultrasonication on ice and centrifugation at 1500×*g* for 10 min, the cell supernatant was incubated with 100 μL of acid reagent at 20–30 °C and centrifuged at 4500×*g* for 10 min. The BCA kit (cat. no. P0012S; Beyotime Biotechnology, Shanghai, China) was used to determine protein concentration. Approximately 100 μL of cell supernatant and 25 μL of 5,5′-dithiobis(2-nitrobenzoic acid) solution were incubated together in a 96-well plate for 5 min at 20–30 °C. The absorbance of each

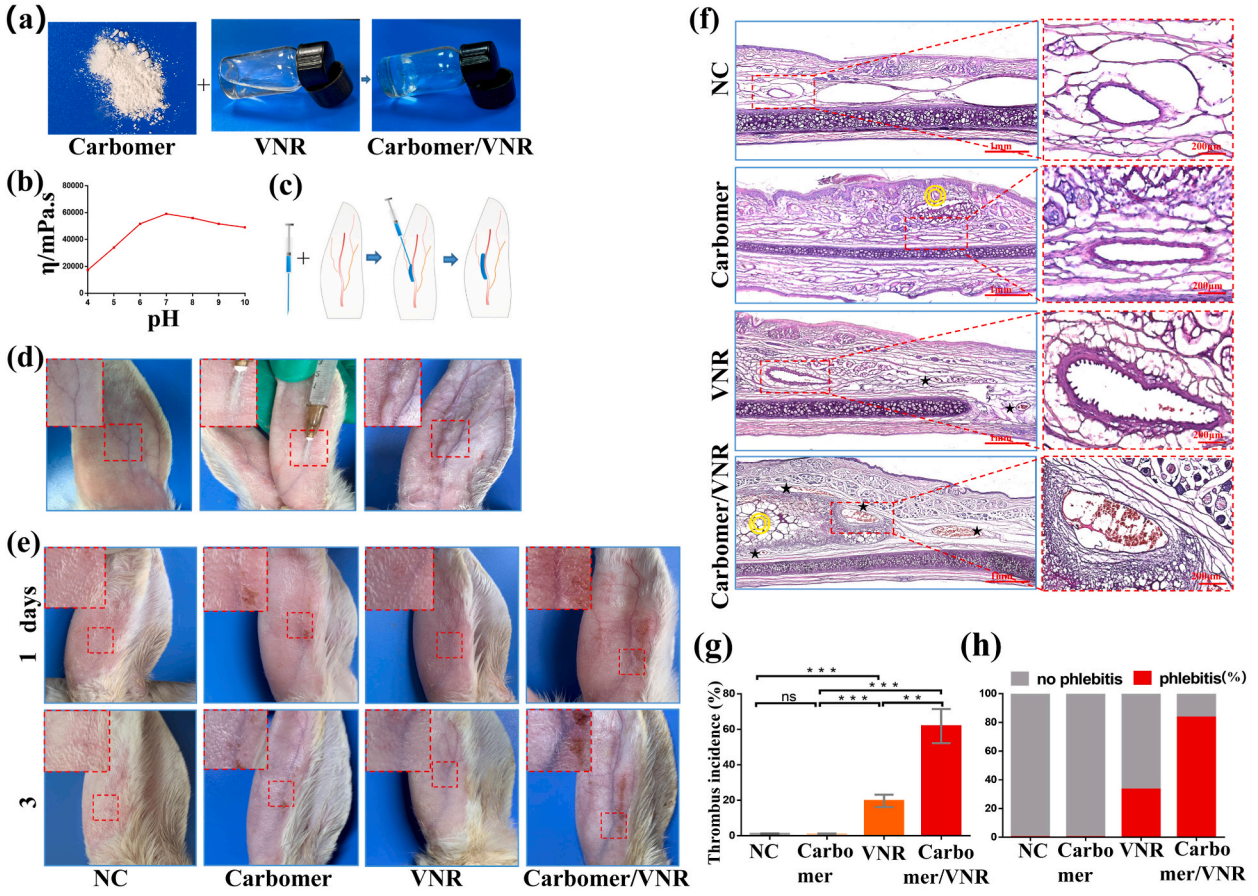

Fig. 1. Carbomer/VNR gel rapidly induces phlebitis in rabbit ear veins. (a) Approximately 0.01 g carbomer, 1 ml deionized water, and 1 ml of VNR (0.6 mg/ml) were mixed to create the carbomer/VNR gel. (b) The viscosity of the carbomer/VNR gel was analyzed at different pH values (4.0, 5.0, 6.0, 7.0, 8.0, 9.0, and 10.0). (c–d) The gel was injected around the veins rather than inside the vessels in rabbits using a syringe. The gel was injected as the needle was withdrawn. The needle gauge was 26G. (e) The morphology of the veins of the rabbit ears in NC (n = 3), carbomer (n = 3), VNR (n = 3), and carbomer/VNR (n = 3) groups was observed on days 1 and 3. (f–h) HE staining, the incidence of thrombus and phlebitis were statistically analyzed. VNR: Vinorelbine ditartrate; ◎ the injection site of the gel; ★ venous thrombus. NC: normal control. ns: $p > 0.05$; *$p < 0.05$; **$p < 0.01$; ***$p < 0.001$.

well was obtained via a microplate reader at 405–414 nm. The amount of GSH in the cells was calculated based on a GSH standard curve and normalized to the protein concentration.

For the MDA assay, the extraction solution (0.5 ml) was added to the cell suspension and ultrasonicated on ice. Subsequently, 0.1 ml of the sample was mixed evenly with 1 ml working solution. After incubation in water at 100 °C for 40 min, the samples were centrifuged at 1078×*g* for 10 min. The BCA kit was used to determine protein concentration. Approximately 250 μL of supernatant was placed in the 96-well plate, and the absorbance of each well at 532 nm was measured using a microplate reader. The MDA levels in each sample were normalized to the protein concentration.

2.9. Lipid peroxidation and reactive oxygen species (ROS) assay

Lipid peroxidation levels were detected via C11-BODIPY™ 581/591 (cat. no. D3861, Thermo Fisher Scientific, Massachusetts, USA). ROS levels were analyzed via CellROX™ Deep Red Flow Cytometry Assay Kit (cat. no. C10491, Thermo Fisher Scientific, Massachusetts, USA). The VECs were digested and isolated using trypsin. The cell precipitate was resuspended after centrifugation at 300×*g* for 5 min. For the lipid peroxidation assay, the cells were incubated with C11-BODIPY 581/591 at 37 °C for 30 min. After washing with PBS, the cells were analyzed using flow cytometry. For ROS assay, the cells were incubated with CellROX™ Deep Red reagent at 37 °C and 5 % CO_2 for 1 h. SYTOX Blue Dead cell staining reagent was added during the last 30 min of incubation. The cells were then washed with PBS and analyzed using flow cytometry.

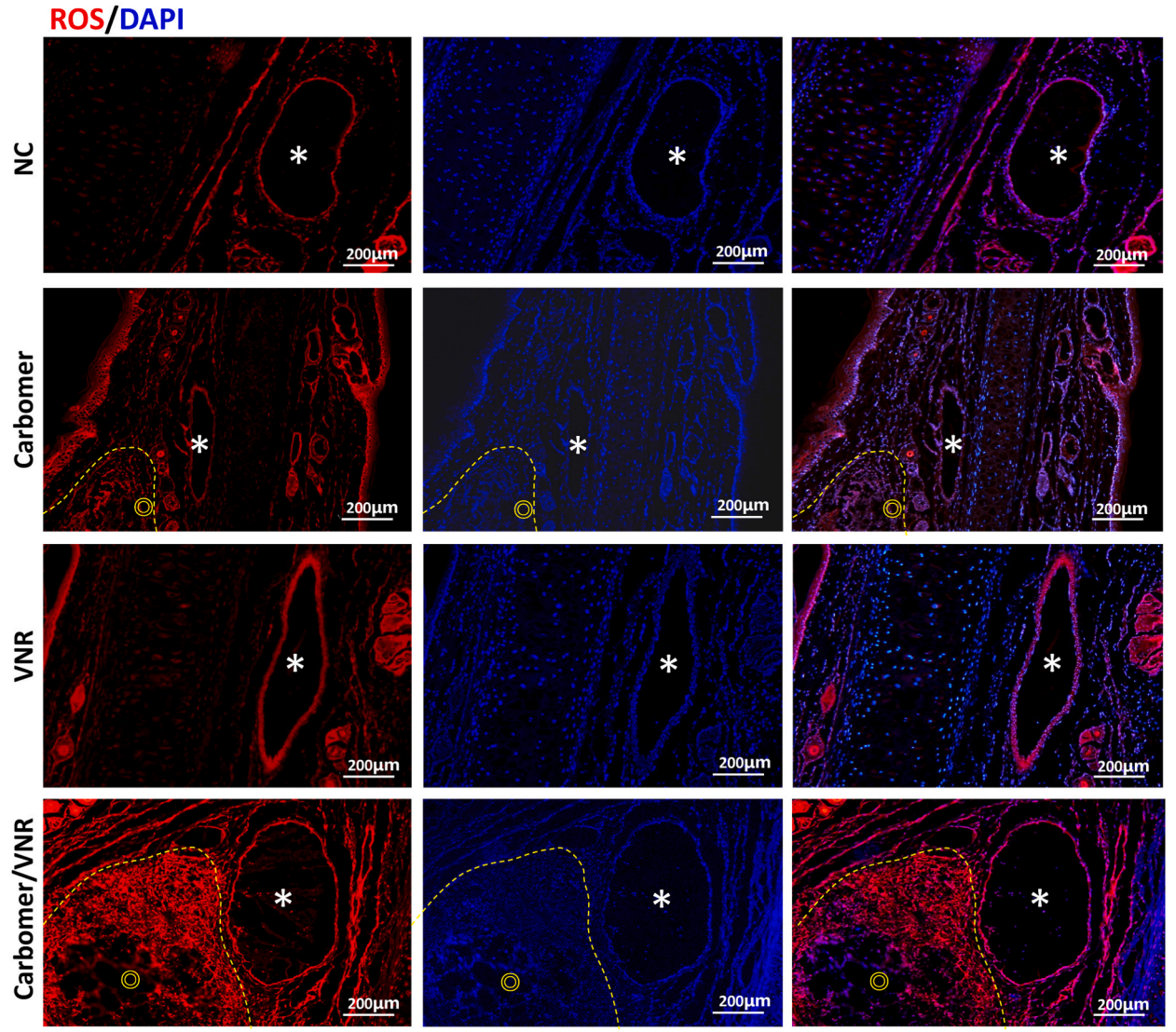

Fig. 2. Carbomer/VNR gel induces oxidative stress in rabbit ear veins. The fluorescence staining of reactive oxygen species (ROS) was detected in the veins of rabbits in the NC, carbomer, VNR, and carbomer/VNR groups. ◎ injection site of the gel; ✱ veins.

2.10. Transmission electron microscopy (TEM)

The tissue samples were fixed with 3 % glutaraldehyde at 4 °C for two days. The samples were then treated with 1 % osmic acid for 30 min. After gradient dehydration with 50–100 % ethanol and immersion in 100 % acetone/Epon 812, ultrathin slices (60 nm) were prepared. The sections were stained with 5 % uranium acetate for 30–60 min and then with lead citrate for 10 min. After drying, the sections were observed using TEM (Philips, Amsterdam, Netherlands).

2.11. Preparation of carbomer, carbomer/VNR, and carbomer/VNR/NAC gel

The carbomer (0.02 g) was added to deionized water (2 ml) for full dissolution. The pH of the carbomer gel was adjusted to approximately 7.0 with 1 mol/L NaOH solution. Vinorelbine ditartrate (VNR, 3 mg) was dissolved in 5 ml PBS using ultrasound to obtain a 0.6 mg/ml VNR stock solution. Subsequently, 1 ml PBS, 1 ml VNR (0.6 mg/ml), or a mixture of 1 ml of VNR (0.6 mg/ml) and NAC (1.2 mM) was added to the 1 ml 1 % carbomer gel to obtain a 0.5 % carbomer gel with a final VNR concentration of 0.3 mg/ml and a NAC concentration of 0.6 mM. The carbomer, carbomer/VNR, and carbomer/VNR/NAC gels were prepared after thoroughly mixing the components. The viscosity of the carbomer/VNR gel was detected using a digital rotational viscometer (SNB-1A, FANGRUI, Shanghai, China) with a #29 rotor at 1 rpm.

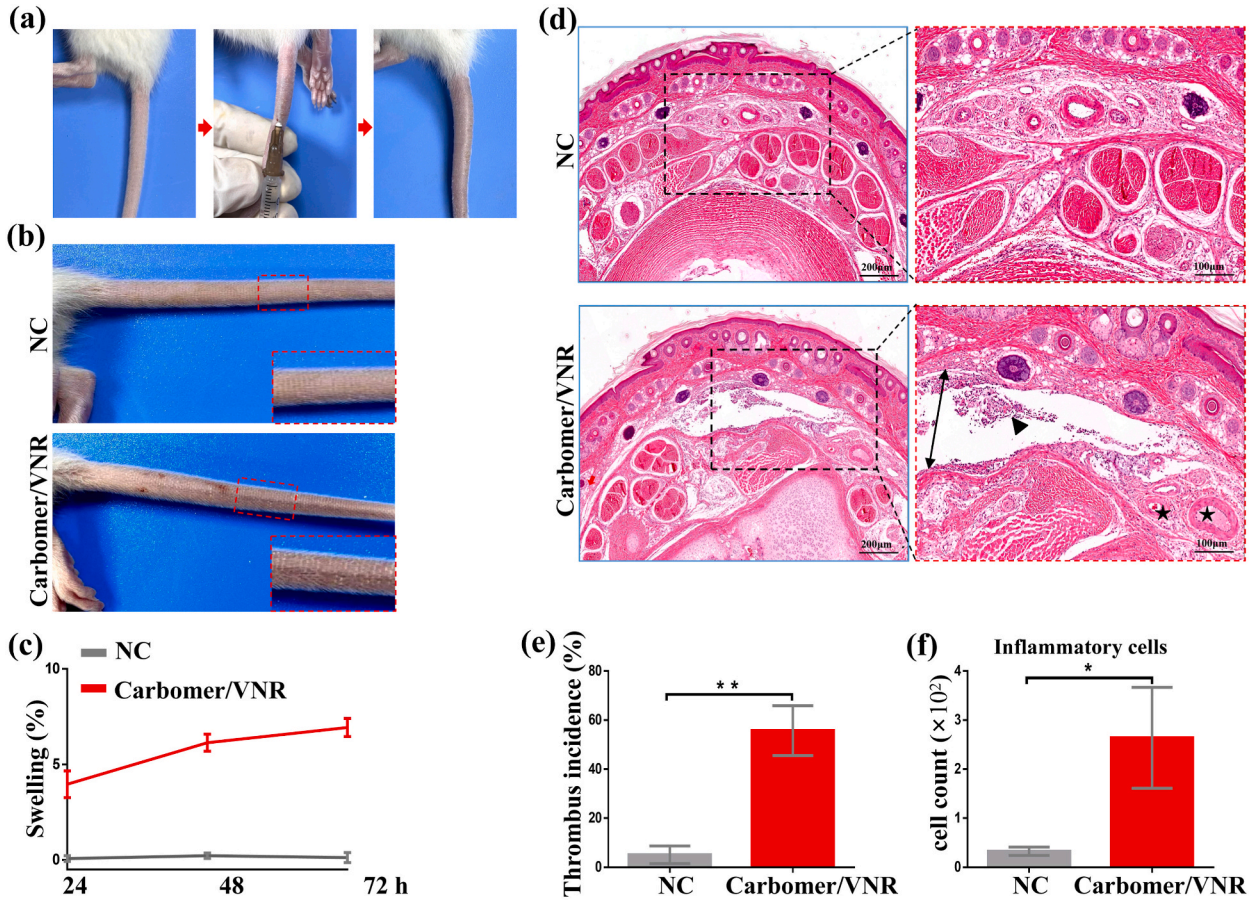

Fig. 3. Carbomer/VNR gel injected around the tail veins rapidly and efficiently induces phlebitis in rats. (a–b) Carbomer/VNR gel was injected around the tail veins, and changes in the tail veins were observed on day 3. (c) The swelling rate of the tails was statistically analyzed at 24, 48, and 72 h after injection. (d–f) HE staining, the incidence of thrombus, and the count of inflammatory cells were statistically analyzed in NC (n = 5) and carbomer/VNR (n = 5) groups. ★ venous thrombus; ↔ edema; ▲ inflammatory cells. NC: normal control. ns: $p > 0.05$; *$p < 0.05$; **$p < 0.01$; ***$p < 0.001$.

2.12. Animal experiments

The rabbits were anesthetized using 3 % sodium pentobarbital (50 mg/kg). Twenty-one 3-month-old New Zealand rabbits (approximately 2–2.5 kg) were used to establish VNR-induced phlebitis and to validate the therapeutic effect of NAC. Twelve rabbits were divided evenly into the normal control (NC), carbomer, VNR, and carbomer/VNR groups to verify the role of carbomer/VNR in the induction of phlebitis. The remaining nine rabbits were divided evenly into the NC, carbomer/VNR, and carbomer/VNR/NAC groups to verify the role of NAC in inhibiting the occurrence of phlebitis. Both ears of the rabbit were used for the corresponding experiments. In the VNR group, VNR (0.3 mg/ml) was injected into the ear vein on day 1. The injection was administered at a rate of 5 ml/kg/h for 30 min. In the carbomer, carbomer/VNR and carbomer/VNR/NAC groups, the rabbits were injected with carbomer, carbomer/VNR, and carbomer/VNR/NAC gels into the tissue between the veins and skin along the direction of the rabbit ear vein. The gel was injected as the needle was withdrawn such that it was retained and wrapped in the vein in situ.

Rats were anesthetized with 3 % sodium pentobarbital (50 mg/kg). VECs were extracted from two three-week-old rats. Twenty-five three-week-old rats (weighing approximately 50–100 g) were used for *in vivo* experiments. Ten rats were divided evenly into normal control (NC) and carbomer/VNR groups to validate the effect of the carbomer/VNR sustained-release carrier on phlebitis. Fifteen rats were divided evenly into the NC, carbomer/VNR, and carbomer/VNR/NAC groups to analyze the inhibitory effects of NAC on VNR-induced phlebitis. In the carbomer/VNR and carbomer/VNR/NAC groups, the carbomer/VNR and carbomer/VNR/NAC gels were injected around the tail veins through a syringe on day 1. Tail diameters near the injection site were measured 0, 24, 48, and 72 h after gel injection. The tail swelling rate was compared with that at 0 h using the formula: Swelling rate (%) = [(diameter of the rat tail at 24, 48, or 72 h − diameter of the rat tail at 0 h)/diameter of the rat tail at 0 h] × 100 %. The incidence of thrombus (%) was measured as (the number of thrombus-containing veins/the total number of veins) × 100 %. The incidence of phlebitis (%) was measured as (the number of phlebitis-containing rabbits' ears/the total number of rabbits' ears) × 100 %. In a transverse section of the tail, the average number of inflammatory cells in three randomly selected fields was counted to estimate the number of inflammatory cells. Animal use

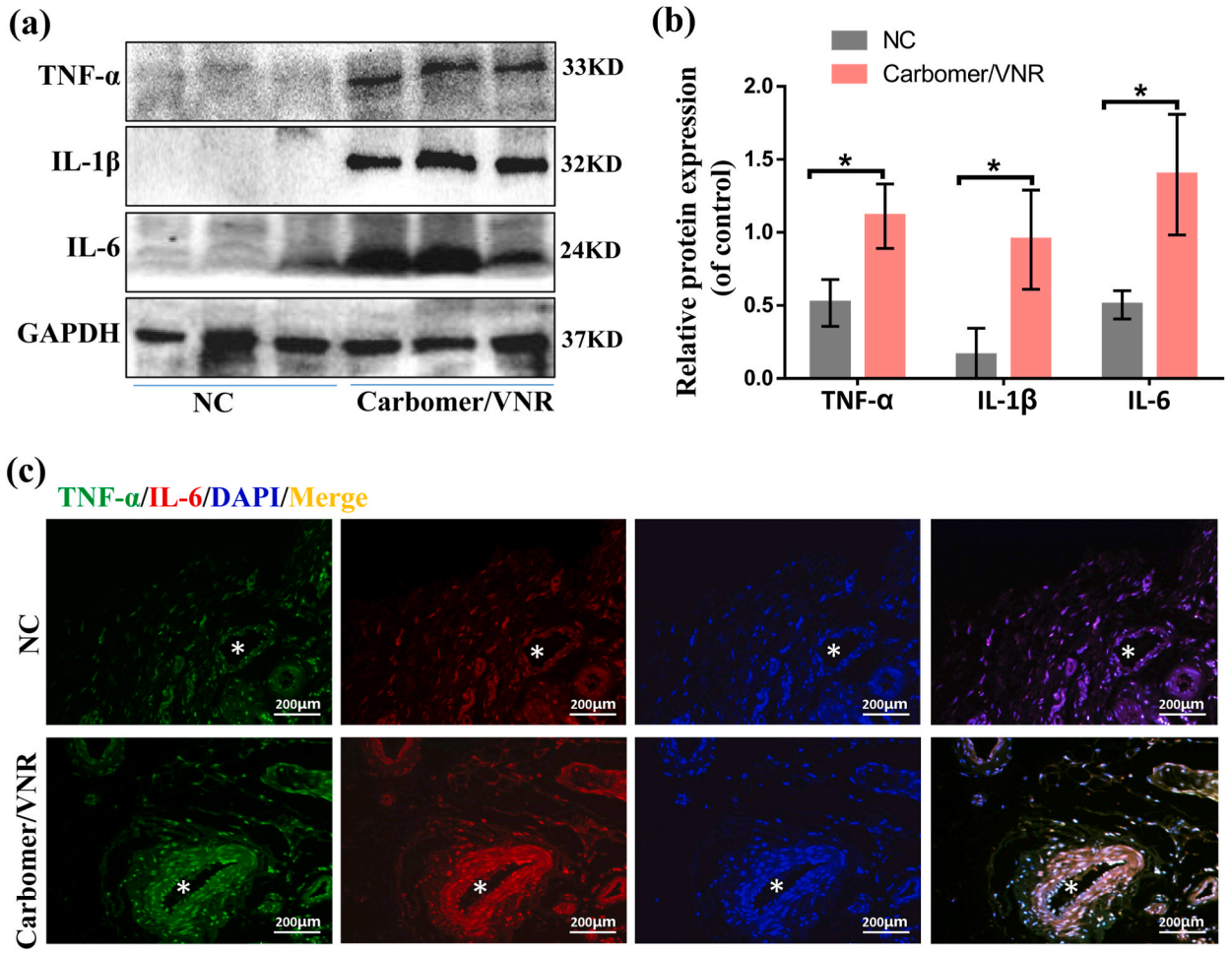

Fig. 4. Carbomer/VNR gel enhances the expression of inflammatory cytokines in rat tail veins. (a–b) Representative western blotting and quantitative data of TNF-α, IL-1β, and IL-6 expression in the tail vein and surrounding tissues of rats treated with NC or carbomer/VNR gel. (c) Representative immunofluorescence staining of TNF-α (green) and IL-6 (red) in the tail vein of rats treated as described earlier. ✱ veins. NC: normal control. ns: $p > 0.05$; *$p < 0.05$. (For interpretation of the references to colour in this figure legend, the reader is referred to the Web version of this article.)

and experimental procedures were approved by the Animal Ethics Committee of the Army Medical University (AMUWEC20230336).

2.13. Statistical analyses

The data are presented as means ± standard deviations on at least three measurements. Student's t-test or one-way analysis of variance was used to analyze the data using SPSS (version 22.0; IBM Corp., NY, USA) or GraphPad Prism (version 7.0; GraphPad Software Inc., CA, USA). Graph analysis was performed using GraphPad Prism version 7.0. Statistical significance was set at $p < 0.05$.

3. Results and discussion

3.1. Carbomer/VNR gel induces phlebitis rapidly and efficiently in rabbits

Phlebitis is caused by the injection of stimulative drugs, such as chemotherapy and hypertonic drugs, through the superficial vein, which damages VECs and causes inflammation of the vein and surrounding tissues [8,26]. Owing to its high incidence, as well as clinical symptoms such as pain and swelling, prevention and treatment strategies for phlebitis are urgently required [5,6,27]. Currently, the establishment of phlebitis models is mainly based on intravascular injections in rabbits and mice [6,11]. However, owing to the difficulty of intravascular injection, phlebitis cannot be induced quickly, simply, or efficiently, thus affecting mechanistic studies and the formulation of prevention strategies against this condition. In this study, we developed an innovative animal model of phlebitis to explore its pathogenesis and develop prevention strategies. VNR and the carbomer were mixed to form a gel (Fig. 1a). The

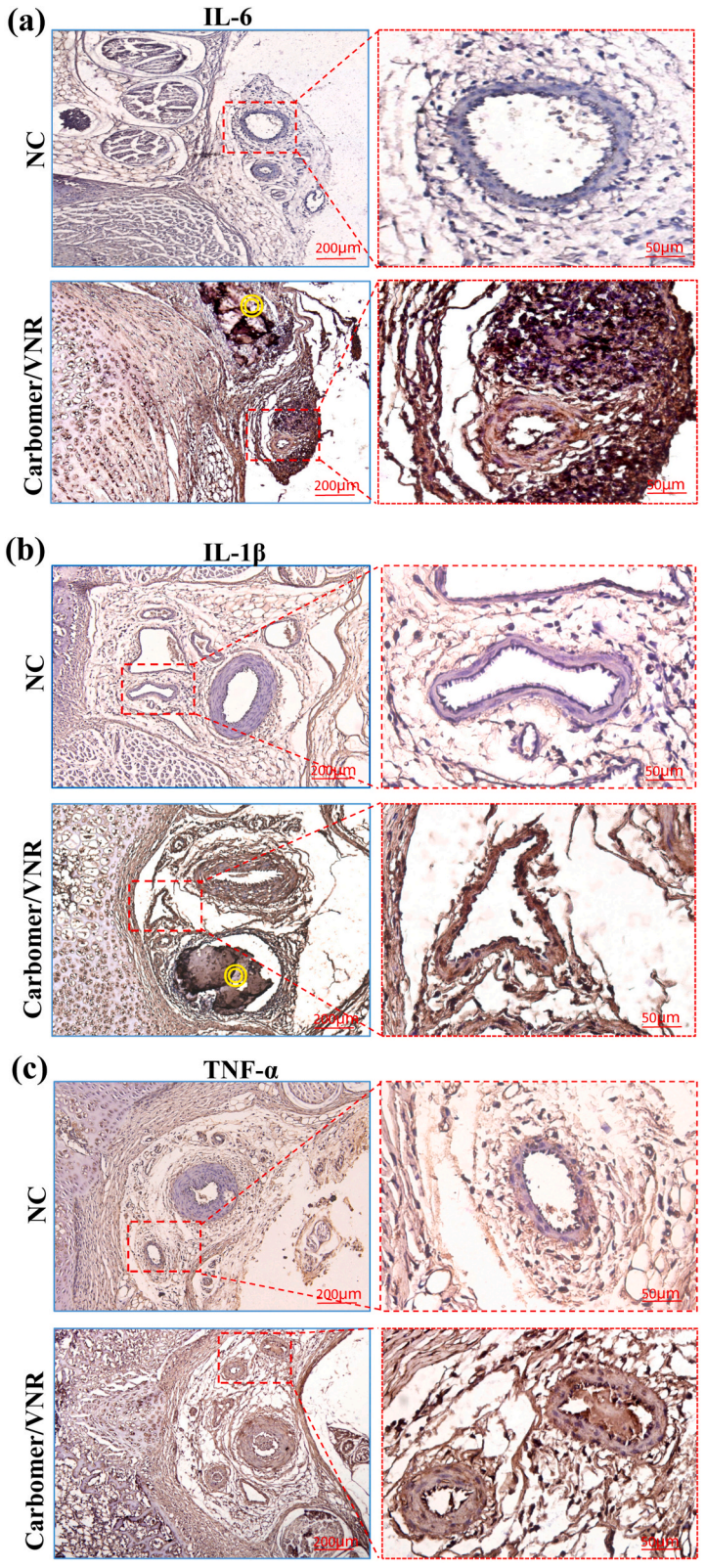

Fig. 5. Carbomer/VNR gel promotes the expression of inflammatory cytokines in the tail vein of rats. (a–c) Representative immunohistochemical staining of IL-6, IL-1β, and TNF-α in NC and carbomer/VNR groups. ◎ the injection site of the gel.

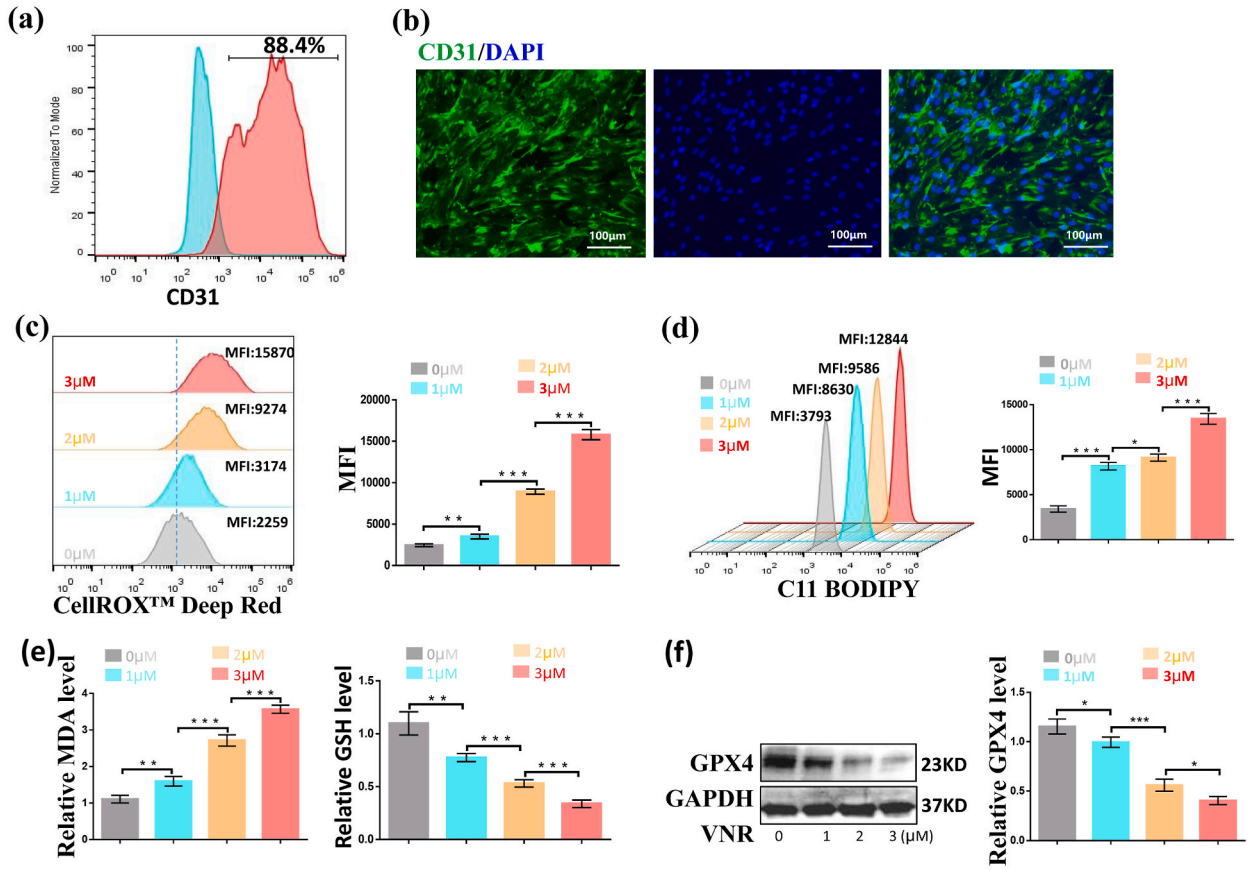

Fig. 6. VNR promotes oxidative stress in venous endothelial cells (VECs). (a) Cell surface marker CD31 of VECs was detected using flow cytometric analysis. The right curve represents the fluorescence intensity of VECs stained with the CD31 antibody. (b) Representative immunofluorescence staining of CD31 (green) in VECs. (c) ROS levels and mean fluorescence intensity (MFI) of VECs treated with different concentrations of VNR (0, 1, 2, and 3 μM). (d) Lipid peroxidation levels and mean fluorescence intensity (MFI) of VECs treated as stated the above. (e) The MDA levels and GSH levels in VECs treated with different concentrations of VNR (0, 1, 2, and 3 μM). (f) Representative western blotting and quantitative data of GPX4 in VECs treated as described earlier. NC: normal control. ns: $p > 0.05$; *$p < 0.05$; **$p < 0.01$; ***$p < 0.001$. (For interpretation of the references to colour in this figure legend, the reader is referred to the Web version of this article.)

viscosity of the carbomer/VNR gel was analyzed at different pH values (4.0, 5.0, 6.0, 7.0, 8.0, 9.0, and 10.0). It was known that the viscosity of the carbomer/VNR gel was the highest (about 60,000 mPa.s) at a pH of 7.0 (Fig. 1b). Then the gel was then injected around the veins in situ. The schematic representation of the experimental workflow is shown as Fig. 1c–d. Rabbit ear veins were observed on days 1 and 3 after treatment with the carbomer gel, VNR, or carbomer/VNR gel. The rabbits in the carbomer and VNR groups did not exhibit significant redness and thickening in the ear veins compared with those in the NC group, whereas the carbomer/VNR gel sustained-release carrier significantly caused redness and thickening of the veins on days 1 and 3 (Fig. 1e). HE staining revealed no significant change in veins in the NC and carbomer groups. Although the venous wall was vacuolated and stratified in the VNR group, several clots were observed in the veins of the carbomer/VNR group (Fig. 1f). Moreover, the incidence of thrombus formation and phlebitis was the highest in the carbomer/VNR group (Fig. 1g–h). ROS levels and oxidative stress were detected, and we observed that the ROS levels in the veins increased significantly in the VNR and carbomer/VNR groups, especially in the carbomer/VNR group (Fig. 2). Collectively, our results suggest that the gel sustained-release carrier loaded with VNR could be retained in situ, wrap around the veins, and facilitate the prolonged release of VNR, acting as an efficient and simple method to induce phlebitis. Considering that severe extravasation and diffusion of chemotherapy agents in the tissues can lead to necrosis of surrounding tissues and skin ulcer [28], we speculate that the sustained-release gel loaded with VNR injected around veins is harmful to the surrounding tissues. Therefore, it may be urgent to prepare the carbomer/VNR sustained-release carrier gel with local retention but degradation quickly to reduce the damage to the surrounding healthy tissues.

3.2. *Carbomer/VNR gel rapidly and efficiently induces phlebitis in rats*

We also injected the carbomer/VNR gel around the tail vein in rats to analyze the effect of the gel sustained-release carrier on inducing phlebitis (Fig. 3a). The tail veins of rats treated with the carbomer/VNR gel were evidently red and thickened (Fig. 3b). The

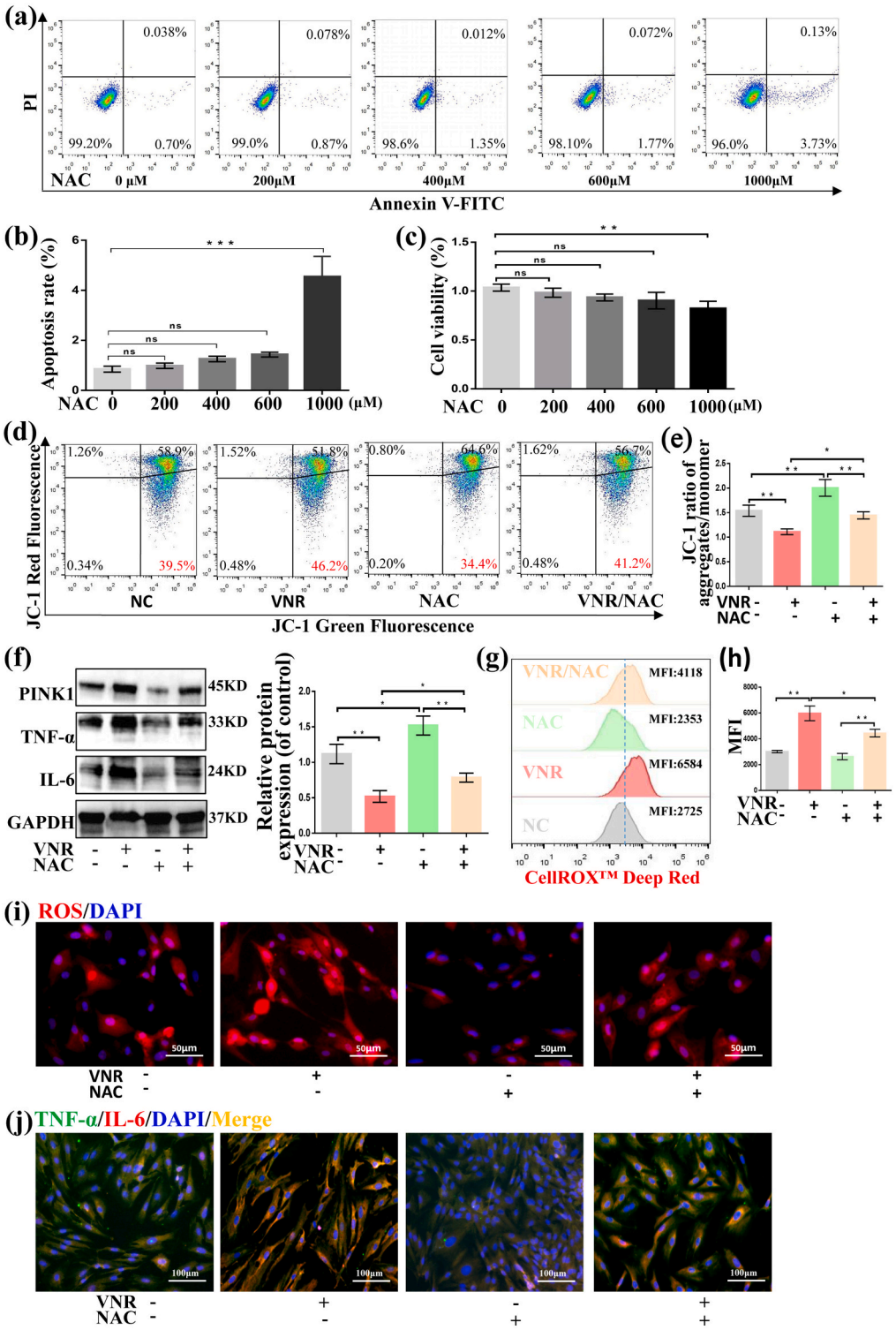

Fig. 7. NAC reduces mitochondrial damage-induced ROS levels and inhibits inflammatory cytokine expression in VECs. (a–b) The apoptosis rate of VECs treated with different concentrations of NAC (0, 200, 400, 600, and 1000 μM) was detected by flow cytometry and then statistically analyzed. (c) Cell viability of VECs treated with different concentrations of NAC (0, 200, 400, 600, and 1000 μM) was detected using CCK-8. (d–e) Mitochondrial membrane potential (MMP) and data analysis of VECs treated with NC, VNR, NAC, and VNR/NAC. In the VNR/NAC group, NAC (600 μM) was pre-treated for 2 h before being added to VNR (2 μM); the detection of MMP and statistical analysis were performed one day later. (f) Representative western blotting and quantitative data of PINK1, TNF-α, and IL-6 in VECs treated as described earlier. (g–j) ROS levels and MFI

analysis, ROS fluorescence staining, and immunofluorescence staining of TNF-α (green) and IL-6 (red) in VECs treated as described earlier. NAC: N-acetylcysteine amide; NC: normal control. ns: $p > 0.05$; *$p < 0.05$; **$p < 0.01$; ***$p < 0.001$. (For interpretation of the references to colour in this figure legend, the reader is referred to the Web version of this article.)

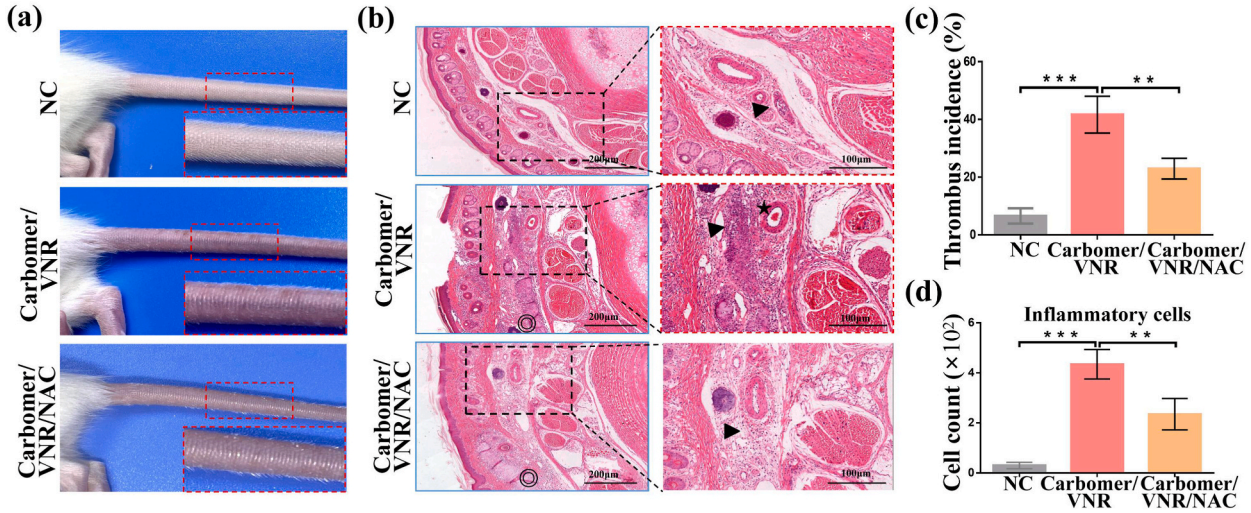

Fig. 8. NAC effectively attenuates carbomer/VNR gel-induced phlebitis in rats. (a) The morphology of the veins on the third day in the NC (n = 5), carbomer/VNR (n = 5), and carbomer/VNR/NAC (n = 5) groups. (b–d) HE staining, the incidence of thrombus, and the count of inflammatory cells were statistically analyzed in the NC, carbomer/VNR, and carbomer/VNR/NAC groups. ◎ the injection site of gel; ★ venous thrombus; ▲ inflammatory cells. NC: normal control. ns: $p > 0.05$; *$p < 0.05$; **$p < 0.01$; ***$p < 0.001$.

swelling rate of the tail increased with time and reached approximately 7 % at 72 h (Fig. 3c). HE staining of the transverse sections of the tail indicated that thrombus formation, the incidence of thrombus, and the number of inflammatory cells in the tail vein were significantly increased in rats treated with the carbomer/VNR gel (Fig. 3d–f). Western blotting analysis revealed increased levels of inflammatory cytokines TNF-α, IL-1β, and IL-6 in the veins and surrounding tissues of rats in the experimental group (Fig. 4a–b). Immunofluorescence staining indicated increased expressions of inflammatory cytokines IL-6 and TNF-a in the veins of rats in the experimental group (Fig. 4c). Immunohistochemical analysis displayed an increased expression of IL-6, IL-1β, and TNF-α in the veins of rats in the carbomer/VNR group compared with that in the NC group (Fig. 5a–c). We continuously stimulated the veins by injecting carbomer/VNR sustained-release carrier gels around them to rapidly and locally induce phlebitis in rats.

3.3. *VNR increases the production of reactive oxygen species in VECs*

Vinorelbine (VNR), a potent antitumor drug that causes venous irritation, plays a crucial role in inducing phlebitis. VNR can also increase the expression of pro-inflammatory cytokines by increasing ROS levels in endothelial cells [6,29]. To analyze the mechanism by which VNR promotes the expression of inflammatory cytokines in VECs, VECs were extracted and identified by flow cytometry and immunofluorescence staining, which also indicated that most of the extracted cells expressed the marker protein CD31 (Fig. 6a–b). The ROS levels and lipid peroxidation levels of VECs treated with different concentrations of VNR (0, 1, 2, and 3 μM) were detected, and quantitative analysis was conducted. With an increase in the VNR concentration, the levels of ROS and lipid peroxidation also increased significantly (Fig. 6c–d). Moreover, compared with VECs treated without VNR, MDA levels increased, and GSH levels decreased significantly in VECs treated with increasing concentrations of VNR (Fig. 6e). Western blotting and quantitative analysis also indicated that VNR reduced the expression of glutathione peroxidase 4 (GPX4), which was associated with the promotion of oxidative stress with increasing VNR concentrations (Fig. 6f). Thus, VNR could increase ROS levels in VECs.

3.4. *NAC reduces mitochondrial damage-induced ROS levels and inhibits the inflammatory response in VECs*

Research has shown that N-acetylcysteine (NAC) amide reduces ROS levels caused by mitochondrial dysfunction [30]. Therefore, the ability of NAC to decrease the levels of pro-inflammatory cytokines by reducing ROS production was monitored. To determine the cytotoxicity of NAC on VECs, the apoptosis rate and cell viability were analyzed. It was observed that NAC was basically non-toxic to cells when its concentration was less than 600 μM. However, when the concentration exceeded 1000 μM, it significantly promoted cell apoptosis and weakened cell viability (Fig. 7a–c). Thus, low concentrations of NAC are needed when using NAC for phlebitis prevention and treatment. By examining mitochondrial membrane potential and statistical analysis of the ratio of aggregates/monomers, we observed that VNR could cause mitochondrial dysfunction, which could be alleviated by NAC (Fig. 7d–e). The results of western blotting and quantitative analysis suggested that VNR could promote the production of PINK1 related to mitochondrial oxidative stress

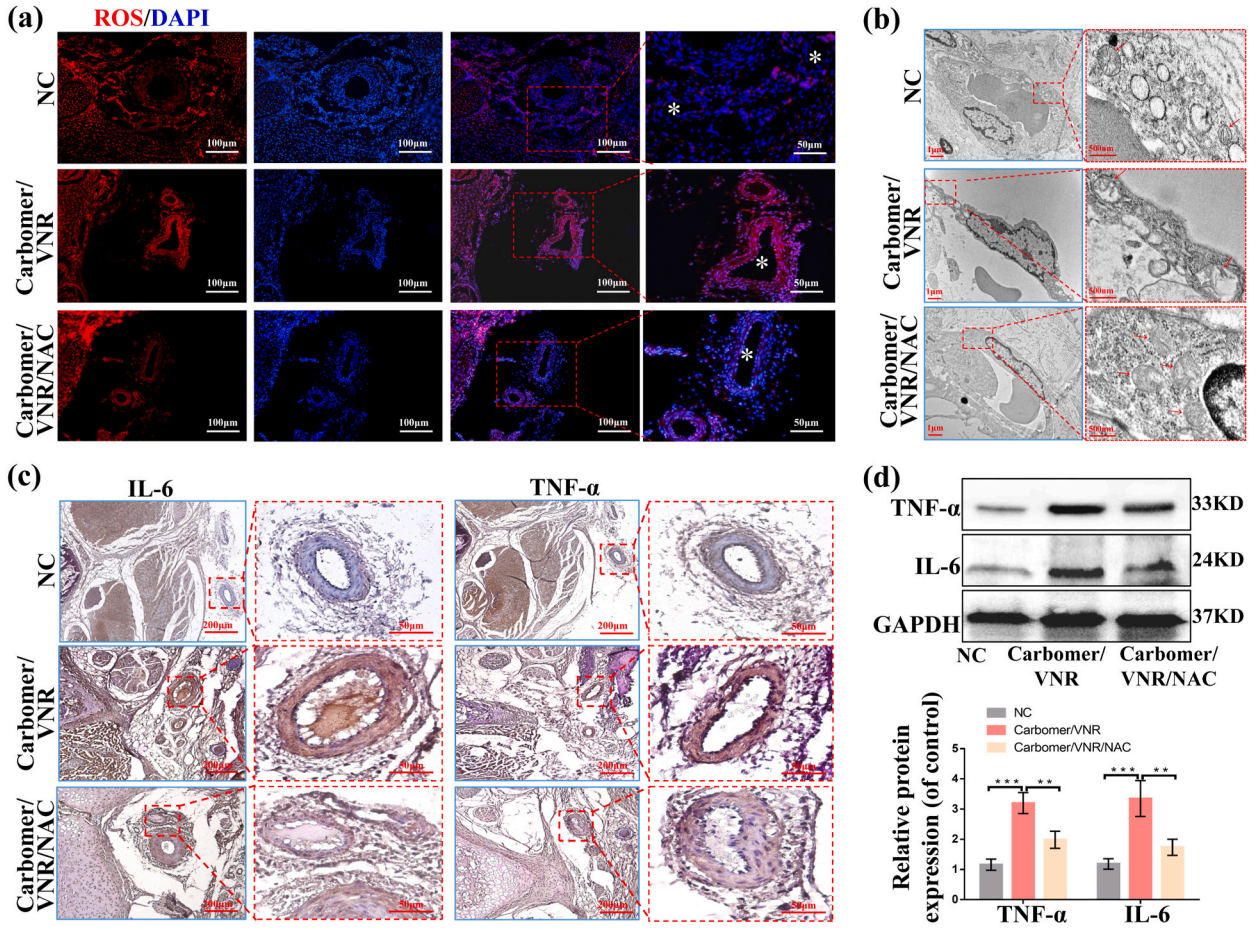

Fig. 9. NAC reduces the incidence of phlebitis by inhibiting the mitochondrial oxidative stress-induced inflammatory responses in rats. (a) ROS fluorescence staining in veins in the NC, carbomer/VNR, and carbomer/VNR/NAC groups. (b) Morphological characteristics of mitochondria in VECs treated as described earlier. (c–d) Representative immunohistochemical staining, western blotting, and quantitative data of IL-6 and TNF-α were monitored in veins and surrounding tissues. → Mitochondria; ✱ veins. NC: normal control. ns: $p > 0.05$; $^{*}p < 0.05$; $^{**}p < 0.01$; $^{***}p < 0.001$.

and increase the expression of inflammatory cytokines, IL-6 and TNF-α, which could also be inhibited by NAC (Fig. 7f). Then, ROS levels and fluorescence intensity were detected using flow cytometry, and the expression of inflammatory cytokines was analyzed using immunofluorescence staining (Fig. 7g–j). Collectively, our findings suggested that VNR could promote the expression of TNF-αand IL-6 by enhancing intracellular oxidative stress and increasing ROS levels, however, NAC could effectively reverse these changes.

3.5. *NAC attenuates carbomer/VNR gel-induced phlebitis in rabbits and rats*

It was known that VNR could induce mitochondrial dysfunction in VECs, resulting in increased ROS levels, which consequently leads to increased levels of the pro-inflammatory cytokines IL-6, TNF-α, and IL-1β. However, prevention of phlebitis after its occurrence owing to the increased ROS levels has not been reported. Growing evidence suggest that mitochondria are the main source of ROS in cells [31,32]. The overproduction of ROS after mitochondrial function injury promotes the expression and release of inflammatory cytokines [32,33]. To validate the inhibitory effect of NAC on the occurrence and development of phlebitis *in vivo*, the rats were divided into NC, carbomer/VNR, and carbomer/VNR/NAC groups. Compared with the NC group, the tail vein in rats in the carbomer/VNR group exhibited redness and thickening. In contrast, these symptoms were significantly relieved in the carbomer/VNR/NAC group compared with that in the carbomer/VNR group (Fig. 8a). HE staining of the transverse sections of the tail indicated that thrombus formation, the incidence of thrombus, and number of inflammatory cells in the tail vein were significantly increased in rats treated with the carbomer/VNR gel, which could be reversed by NAC (Fig. 8b–d). Moreover, ROS levels in the tail vein of the carbomer/VNR group increased. In contrast, ROS levels in the tail vein were significantly lower in the carbomer/VNR/NAC group than in the carbomer/VNR group (Fig. 9a). Mitochondrial morphology in VECs indicated that carbomer/VNR caused mitochondrial swelling and cristae reduction, whereas NAC alleviated these effects (Fig. 9b). The results of immunohistochemical staining, western blotting, and quantitative analysis in rats suggested that carbomer/VNR could increase the expression of the inflammatory

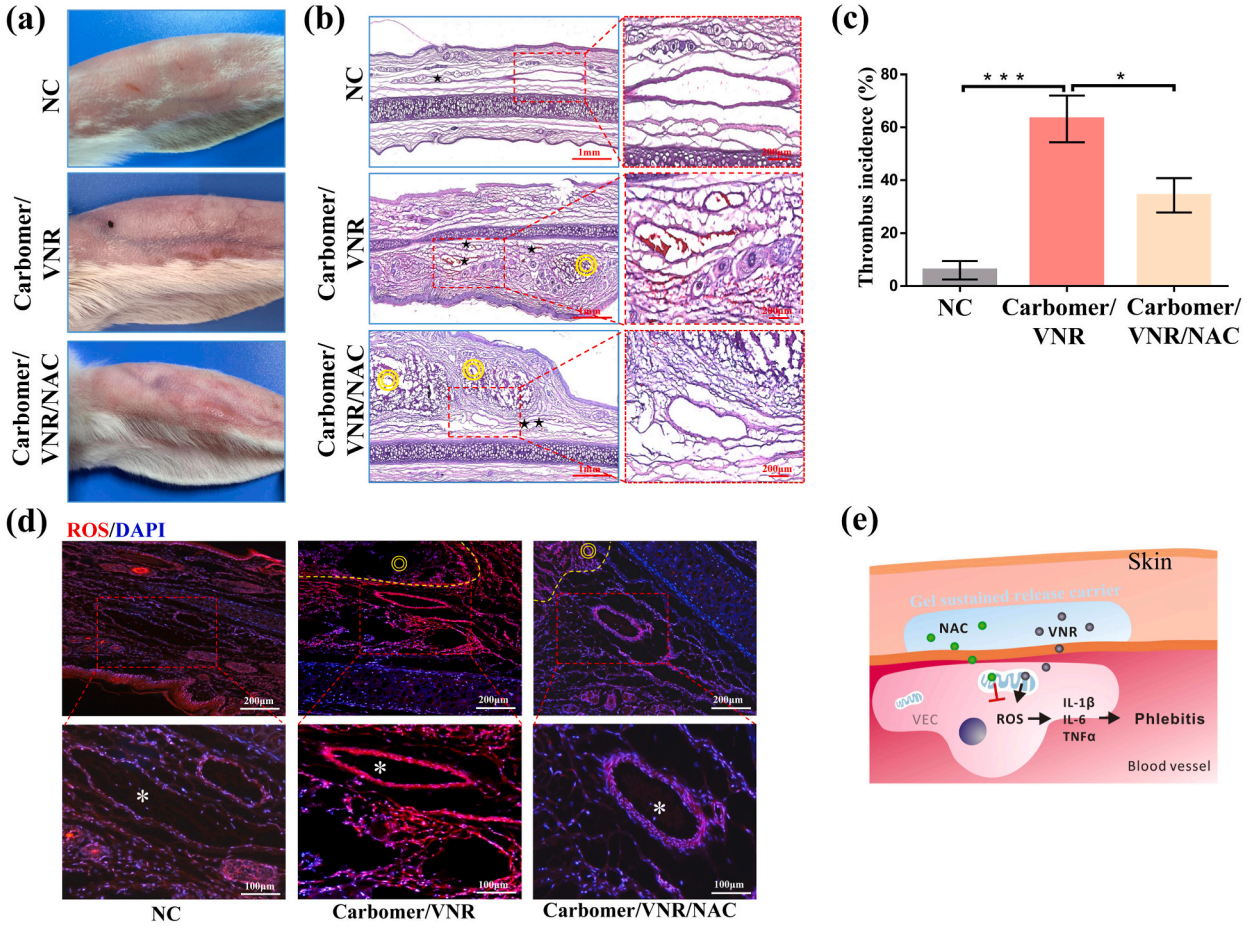

Fig. 10. NAC effectively reverses carbomer/VNR gel-induced phlebitis in rabbits. (a) The morphology of the veins on the third day in the NC (n = 3), carbomer/VNR (n = 3), and carbomer/VNR/NAC (n = 3) groups. (b–c) HE staining and the incidence of thrombus were statistically analyzed in the NC, carbomer/VNR, and carbomer/VNR/NAC groups. (d) ROS fluorescence staining in veins treated as described earlier. (e) Illustration of postulated mechanism by which NAC reduced ROS levels to inhibit the phlebitis induced by the gel sustained-release carrier loaded with VNR. ◎ the injection site of gel; ★ venous thrombus; ✱ veins. NC: normal control. ns: $p > 0.05$; *$p < 0.05$; **$p < 0.01$; ***$p < 0.001$.

cytokines IL-6 and TNF-α, which could also be inhibited by NAC *in vivo* (Fig. 9c–d).

The ear vein of rabbits in the carbomer/VNR group revealed increased redness and thickening compared with that observed in rabbits in the NC group. In contrast, these symptoms were significantly relieved in the carbomer/VNR/NAC group compared with that in the carbomer/VNR group (Fig. 10a). HE staining and statistical analysis of thrombus incidence suggested that carbomer/VNR increased the rate of venous thrombosis, which was reduced by NAC (Fig. 10b–c). Fluorescence analysis also suggested that NAC reversed the VNR-induced increase in ROS levels *in vivo* (Fig. 10d). This indicated that NAC could be administered in advance or simultaneously with chemotherapy drugs to prevent or treat phlebitis in clinical practice. Thus, as shown in Fig. 10e, this study aimed to develop an animal model of phlebitis by constructing a sustained-release carrier gel loaded with VNR and to evaluate the preventive and therapeutic effects of NAC on phlebitis via attenuating mitochondrial damage to reduce reactive oxide species levels and the expression of IL-6, TNF-α, and IL-1β.

4. Conclusions

In this study, VNR and carbomers were mixed to form a carbomer/VNR gel-sustained release carrier loaded with VNR. By simulating the pathological process in which VNR accumulates around venous vessels and stimulates the veins and surrounding tissues to cause phlebitis, a gel-sustained carrier was injected around the venous vessels rather than inside the vessels. Next, we successfully established an animal model of phlebitis by injecting the carbomer/VNR sustained-release carrier gel and demonstrated that NAC could inhibit the occurrence of phlebitis by reducing ROS production *in vitro* and *in vivo* through the alleviation of mitochondrial damage. Our findings provide a rapid and simple method to establish an animal phlebitis model, which would facilitate further investigation into the pathological mechanisms of phlebitis, and also serve as a novel and efficacious method to prevent and treat phlebitis. However, there are also limitations of the study. The degradation rate of the gel in tissues is unclear. And long-term retention

of sustained-release carrier gel may have harmful effects on surrounding tissues. Therefore, in the following study, we need to further prepare sustained-release carrier gel with degradation quickly and less damage to the surrounding tissues.

Authorship contributions

Hongyu Zhang: Conceived and designed the experiments; Wrote the paper; Performed the experiments. Jing Gong: Conceived and designed the experiments; Performed the experiments. Shiyu Zhang: Performed the experiments; Analyzed and interpreted the data; Wrote the paper. Liwen Luo: Performed the experiments; Analyzed and interpreted the data. Ke Bi: Analyzed and interpreted the data. Lei Wang: Contributed reagents, materials, analysis tools or data. Chengqin Luo: Contributed reagents, materials, analysis tools or data. XueWei Kan: Analyzed and interpreted the data. Zhiqiang Tian: Conceived and designed the experiments; Contributed reagents, materials, analysis tools or data; Wrote the paper. Xiaolong Wang: Conceived and designed the experiments; Contributed reagents, materials, analysis tools or data; Wrote the paper.

Data availability

Data will be made available on request.

Institutional review board statement

Animal use and experimental procedures were approved by the Animal Ethics Committee of the Army Medical University (AMUWEC20230336).

Declaration of competing interest

The authors declare that they have no known competing financial interests or personal relationships that could have appeared to influence the work reported in this paper.

Acknowledgements

We would like to thank the Army Medical University Animal Center for providing laboratory animals and Editage (www.editage.cn) for English language editing. This work was supported by the Nanan District Science and Health Joint Medical Research Project Fund (Grant Number: 2021-06).

Appendix A. Supplementary data

Supplementary data to this article can be found online at https://doi.org/10.1016/j.heliyon.2023.e21235.

References

[1] R.M. van Stein, A. Aalbers, G.S. Sonke, W.J. van Driel, Hyperthermic intraperitoneal chemotherapy for ovarian and colorectal cancer: a review, JAMA Oncol. 7 (2021) 1231–1238.
[2] M. Di Nisio, F. Peinemann, E. Porreca, A.W. Rutjes, Treatment for superficial infusion thrombophlebitis of the upper extremity, Cochrane Database Syst. Rev. 2015 (2015), D11015.
[3] L.M. Kaminskas, V.M. McLeod, C.J. Porter, B.J. Boyd, Association of chemotherapeutic drugs with dendrimer nanocarriers: an assessment of the merits of covalent conjugation compared to noncovalent encapsulation, MOL PHARMACEUT 9 (2012) 355–373.
[4] S. Kumar, A. Bajaj, Advances in self-assembled injectable hydrogels for cancer therapy, BIOMATER SCI-UK 8 (2020) 2055–2073.
[5] J.T. Lee, M.A. Kalani, Treating superficial venous thrombophlebitis, J. Natl. Compr. Cancer Netw. : JNCCN. 6 (2008) 760–765.
[6] P. Liu, L. Ye, Y. Ren, et al., Chemotherapy-induced phlebitis via the GBP5/NLRP3 inflammasome axis and the therapeutic effect of aescin, BRIT J PHARMACOL 180 (2023) 1132–1147.
[7] E. Kohno, S. Murase, K. Matsuyama, N. Okamura, Effect of corticosteroids on phlebitis induced by intravenous infusion of antineoplastic agents in rabbits, Int. J. Med. Sci. 6 (2009) 218–223.
[8] G.F. Ge, W.W. Shi, C.H. Yu, et al., Baicalein attenuates vinorelbine-induced vascular endothelial cell injury and chemotherapeutic phlebitis in rabbits, TOXICOL APPL PHARM 318 (2017) 23–32.
[9] J. Zhang, J. Shen, W. Yin, X. Wei, L. Wu, H. Liu, The intervention research on treatment by Xianchen to rabbits model of chemotherapeutic phlebitis, Acta Cir. Bras. 31 (2016) 549–556.
[10] Z. Wang, L. Ma, X. Wang, et al., Cimetidine attenuates vinorelbine-induced phlebitis in mice by militating E-selectin expression, CANCER CHEMOTH PHARM 74 (2014) 239–247.
[11] G.H. Zheng, L. Yang, H.Y. Chen, J.F. Chu, L. Mei, Aloe vera for prevention and treatment of infusion phlebitis, Cochrane Database Syst. Rev. 2014 (2014) D9162.
[12] D.G. Maki, M. Ringer, Risk factors for infusion-related phlebitis with small peripheral venous catheters. A randomized controlled trial, ANN INTERN MED 114 (1991) 845–854.
[13] H.J. Raatschen, Y. Fu, V. Rogut, et al., [Effects of MRI-assayed microvascular permeability on the accumulation of vinorelbine in xenograft tumors], Röfo : Fortschritte dem Geb. Rontgenstrahlen Nukl. 182 (2010) 133–139.
[14] M. Regenold, K. Kaneko, X. Wang, et al., Triggered release from thermosensitive liposomes improves tumor targeting of vinorelbine, J. Contr. Release : official journal of the Controlled Release Society 354 (2023) 19–33.

[15] C. Mouchard-Delmas, I. Devie-Hubert, J. Dufer, Effects of the anticancer agent vinorelbine on endothelial cell permeability and tissue-factor production in man, J. Pharm. Pharmacol. 48 (1996) 951–954.
[16] J. Zhang, N. Tong, Y. Chen, P. Li, S. Yang, X. Zhao, Resveratrol protects against vinorelbine-induced vascular endothelial cell injury, TOXICOL MECH METHOD 23 (2013) 665–671.
[17] C.K. Das, A. Gogia, Vinorelbine-induced chemotherapy port extravasation, Lancet Oncol. 17 (2016) e568.
[18] K. Yoh, S. Niho, K. Goto, et al., High body mass index correlates with increased risk of venous irritation by vinorelbine infusion, Jpn. J. Clin. Oncol. 34 (2004) 206–209.
[19] J. Garcia-Expósito, J. Sánchez-Meca, J.A. Almenta-Saavedra, L. Llubes-Arrià, A. Torné-Ruiz, J. Roca, Peripheral venous catheter-related phlebitis: a meta-analysis of topical treatment, Nursing open 10 (2023) 1270–1280.
[20] H. Nasr, J.M. Scriven, Superficial thrombophlebitis (superficial venous thrombosis), BMJ (Clinical research ed.) 350 (2015) h2039.
[21] T. Yamada, N. Egashira, M. Imuta, et al., Role of oxidative stress in vinorelbine-induced vascular endothelial cell injury, Free Radic. Biol. Med. 48 (2010) 120–127.
[22] Q. Xiao, G. Chen, Y.H. Zhang, F.Q. Chen, H.F. Weng, A.F. Xiao, Agarose stearate-carbomer as stabilizer and rheology modifier for surfactant-free cosmetic formulations, Mar. Drugs 19 (2021).
[23] Y. Huang, F. Shi, L. Wang, et al., Preparation and evaluation of Bletilla striata polysaccharide/carboxymethyl chitosan/Carbomer 940 hydrogel for wound healing, Int. J. Biol. Macromol. 132 (2019) 729–737.
[24] G.F. Rushworth, I.L. Megson, Existing and potential therapeutic uses for N-acetylcysteine: the need for conversion to intracellular glutathione for antioxidant benefits, Pharmacol. Therapeut. 141 (2014) 150–159.
[25] M.A. Zayed, X. Wei, K.M. Park, et al., N-Acetylcysteine accelerates amputation stump healing in the setting of diabetes, Faseb. J. : official publication of the Federation of American Societies for Experimental Biology 31 (2017) 2686–2695.
[26] T. Singh, A. Azim, Administration of 3% hypertonic saline via peripheral route: is it really safe? Am. J. Emerg. Med. 66 (2023) 172–173.
[27] N. Marsh, G. Mihala, G. Ray-Barruel, J. Webster, M.C. Wallis, C.M. Rickard, Inter-rater agreement on PIVC-associated phlebitis signs, symptoms and scales, J. Eval. Clin. Pract. 21 (2015) 893–899.
[28] O. Keritam, V. Juhasz, C. Schöfer, et al., Determination of extravasation effects of nal-iri and trabectedin and evaluation of treatment options for trabectedin extravasation in a preclinical animal model, Front. Pharmacol. 13 (2022), 875695.
[29] K.L. Tsai, P.H. Huang, C.L. Kao, et al., Aspirin attenuates vinorelbine-induced endothelial inflammation via modulating SIRT1/AMPK axis, Biochem. Pharmacol. 88 (2014) 189–200.
[30] Q. Li, J. Liao, W. Chen, et al., NAC alleviative ferroptosis in diabetic nephropathy via maintaining mitochondrial redox homeostasis through activating SIRT3-SOD2/Gpx4 pathway, Free Radic. Biol. Med. 187 (2022) 158–170.
[31] J. Dan Dunn, L.A. Alvarez, X. Zhang, T. Soldati, Reactive oxygen species and mitochondria: a nexus of cellular homeostasis, Redox Biol. 6 (2015) 472–485.
[32] X. Chen, X. Li, W. Zhang, et al., Activation of AMPK inhibits inflammatory response during hypoxia and reoxygenation through modulating JNK-mediated NF-κB pathway, Metab., Clin. Exp. 83 (2018) 256–270.
[33] Q. Lin, S. Li, N. Jiang, et al., PINK1-parkin pathway of mitophagy protects against contrast-induced acute kidney injury via decreasing mitochondrial ROS and NLRP3 inflammasome activation, Redox Biol. 26 (2019), 101254.